

Seismic Response of RC Bridge Piers Considering Soil-Pile Interaction

Takeshi Maki¹, Hiroshi Mutsuyoshi² and Anawat Chotesuwan³

Synopsis: After the Kobe earthquake in 1995 in Japan, many reinforced concrete (RC) bridge piers have been strengthened using various techniques, such as steel jacketing and concrete jacketing. It is anticipated that, when the next strong earthquake comes, foundations will possibly be damaged because of the enhanced capacity of the pier. In this paper, the seismic response of reinforced concrete (RC) bridge piers and foundations were evaluated using the substructure pseudo-dynamic (S-PSD) testing method for cases in which strengthening was provided to the pier and foundation. The S-PSD testing method for bridge pier-foundations was first developed. Based on the developed method, damage in a foundation that supported a strengthened pier was investigated through a pier specimen loading. In addition, the response of a strengthened bridge pier with a strengthened foundation was also examined through a foundation specimen loading. The possibility of foundation damage due to pier strengthening and the effectiveness of foundation strengthening were finally confirmed.

Keywords: substructure pseudo-dynamic test; RC bridge pier; pile foundation; seismic response; seismic strengthening; soil-structure interaction; earthquake

INTRODUCTION

In general capacity design concept, bridge pier supported by foundation is usually designed to have less capacity than that of foundation so that a ductile plastic hinge introduced at the bottom of the pier can absorb input seismic energy. Damage in foundation is avoided as much as possible because it is hard to be inspected and repaired after earthquakes, taking into account the easy accessibility and prompt repair to the plastic hinge in the pier. In the 1995 Great Hanshin (Kobe) Earthquake, severe damage was caused to many bridges due to the lack of sufficient capacity and ductility. After the earthquake, many of them have been reconstructed or strengthened in order to achieve both higher capacity and ductility using various techniques [1,2]. However, with an enhancement in the pier capacity, the possibility can be pointed out that the position of failure may shift from the pier down to the foundation. An urgent and detailed investigation to clarify this matter is needed based on the consideration of soil-structure interaction [3]. There exists an example of the investigation of damage in a structural foundation [4]; however, a more detailed investigation of real-scale bridge piers and foundations is important. In this paper, seismic response of reinforced concrete (RC) bridge piers and foundations were evaluated using the substructure pseudo-dynamic (S-PSD) testing method for cases in which strengthening was provided to the pier and foundation.

RESEARCH SIGNIFICANCE

There were few studies on the influence of seismic strengthening of the pier on the response of the structural foundation. In this paper, the S-PSD test method for a bridge system including soil-structure

¹ Associate Professor of Saitama University, Japan. He received his BS, MS and PhD from the University of Tokyo. His research interests include static and dynamic mechanical behavior of RC and steel-concrete hybrid structures.

² Professor of Saitama University, Japan. FACI Member. He received his doctoral degree in Engineering from the University of Tokyo. He is a member of ACI Committee 440 (Fiber-Reinforced Polymer Reinforcement) and the ACI International Forum as a representative of JCI. His research interests include seismic behavior of RC structures, strengthening of RC members and application of FRP to civil engineering structures.

³ Former graduate student of Saitama University, Japan, where he received his Ph.D.

interaction was developed and the method was applied to the quantitative evaluation of damage level and location in the bridge system. The authors believe that the proposed testing method can be widely applied to investigate the seismic response of a bridge system including structural components of which mechanical behavior is unclear. Further, the results in this paper may contribute to the appropriate and rational strengthening design of existing bridges.

SUBSTRUCTURE PSEUDO-DYNAMIC (S-PSD) TESTING METHOD

The pseudo-dynamic test, which combines advantages of experiment and numerical simulation, has been improved over tens of years. The sub-structuring technique has enabled the investigation of the response of the whole structural system by conducting a loading test on a target structural component. In this research, at first, the S-PSD test method for the superstructure-pier-foundation system was developed, based on a simplified 3 degrees-of-freedom (DOF) model. S-PSD testing method itself has been applied to various dynamic structural problems of multi-DOF system consists of members or components with unknown dynamic characteristics, whereas a simple PSD test method has been developed for single-DOF structural system. The proposed method in this paper was assembled with the same mathematical algorithm as applied in the existing S-PSD test; however, it is the originality of the current method to be emphasized that the behaviors of two components in the target system were acquired from a loading test of single specimen.

Superstructure-Pier-Pile Foundation System as a 3-DOF Model

The response behavior of the system subjected to ground seismic excitation was evaluated using a simplified 3-DOF model as shown in Figure 1. The model consisted of two lumped masses, two translational springs (pier, sway) and one rotational spring (rocking). A ground seismic excitation was input to the fixed end of the sway spring, at the location of the horizontal ground displacement u_g . The global translational and rotational displacements u_1 , u_2 and u_3 at the two lumped masses were converted to the local spring displacements u_p , u_s and u_r , and then they were converted to the restoring forces R_p , R_s and R_r for solving the equation of motion of the system.

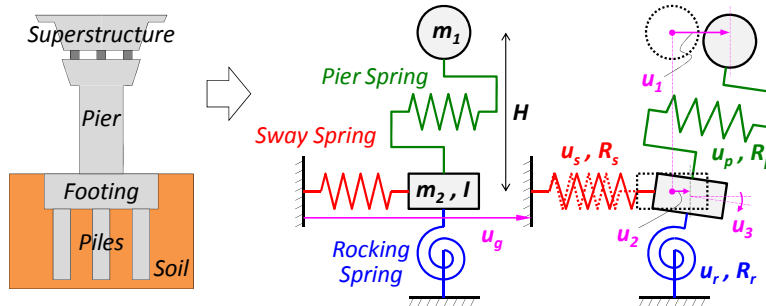


Figure. 1. 3-DOF model for superstructure-pier-foundation system.

Governing Equations and Calculation Algorithm

An equation of motion of the target 3-DOF system in global coordinate can be given as Eq. (1):

$$[M]\{\ddot{u}\} + [C]\{\dot{u}\} + \{R\} = -[M]\{v\}\ddot{u}_g \quad (1)$$

$$[M] = \begin{bmatrix} m_1 & 0 & 0 \\ 0 & m_2 & 0 \\ 0 & 0 & I \end{bmatrix} \quad \{v\} = \begin{Bmatrix} 1 \\ 1 \\ 0 \end{Bmatrix}$$

where m_1 and m_2 are lumped masses of the superstructure and foundation footing, respectively. I is the moment of inertia of the footing and \ddot{u}_g is the ground acceleration at the footing level. $\{\ddot{u}\}$ and $\{\dot{u}\}$ are the global displacement and velocity vectors of the system, respectively. $\{R\}$ is the global restoring force vector of the system.

In order that displacements and forces of the springs are incorporated to the system response, the local vectors are converted to the global vectors through Eqs. (2) and (3):

$$\{u\} = \begin{Bmatrix} u_1 \\ u_2 \\ u_3 \end{Bmatrix} = \begin{Bmatrix} u_p + u_s + u_r H \\ u_s \\ u_r \end{Bmatrix} = \begin{bmatrix} 1 & 1 & H \\ 0 & 1 & 0 \\ 0 & 0 & 1 \end{bmatrix} \begin{Bmatrix} u_p \\ u_s \\ u_r \end{Bmatrix} = \begin{bmatrix} 1 & -1 & -H \\ 0 & 1 & 0 \\ 0 & 0 & 1 \end{bmatrix}^{-1} \{u_L\} \quad (2)$$

$$\{R\} = \begin{Bmatrix} R_1 \\ R_2 \\ R_3 \end{Bmatrix} = \begin{Bmatrix} R_p \\ R_s - R_p \\ R_r - R_p H \end{Bmatrix} = \begin{bmatrix} 1 & 0 & 0 \\ -1 & 1 & 0 \\ -H & 0 & 1 \end{bmatrix} \begin{Bmatrix} R_p \\ R_s \\ R_r \end{Bmatrix} = \begin{bmatrix} 1 & -1 & -H \\ 0 & 1 & 0 \\ 0 & 0 & 1 \end{bmatrix}^T \{R_L\} \quad (3)$$

where, $\{u_L\}$ and $\{R_L\}$ are the local displacement and restoring force vectors, respectively[5].

The governing equation can be numerically solved with application of the Predictor-Corrector method as shown in Figure 2. A predictor displacement calculated by numerical time integration of responses at step n is given to the test specimen or the numerical restoring force model, and then a predictor restoring force can be obtained. The predictor displacement and restoring force are converted to the corrector displacement and restoring force by the Operator Splitting Method [6]. Response acceleration at step $n+1$ is finally given by solving the instantaneous equation of motion.

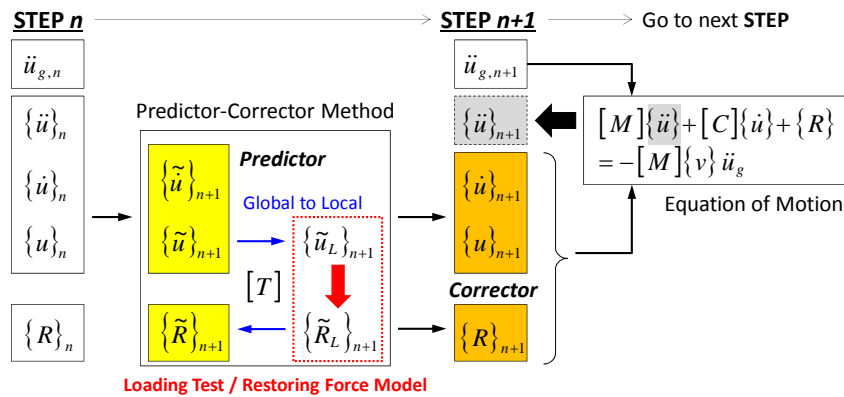


Figure. 2. Calculation algorithm for numerical solution of equation of motion in S-PSD test.

Target Structure: Highway Bridge Pier

The typical RC highway bridge pier in Japan, as shown in Figure 3, was selected as a target structure in this study. The bridge pier and foundation were designed according to the Japanese specification for earthquake-resistant design code of highway bridges (1971)[7]. The design code had been applied to the major number of bridges in Japan before the 1995 Kobe Earthquake occurred. Because of a lack of lateral capacity, the bridge piers designed by the code have been strengthened by the concrete jacketing technique, as shown in Figure 3. The figure also contains a soil profile at the construction site. Table 1 shows calculated capacities of the pier before and after strengthening. The upgrade ratios of flexural and shear capacities by the concrete jacketing were 1.53 and 2.64, respectively. The capacity ratio of foundation to pier reduced from 1.70 to 1.11 due to the increase of pier flexural capacity.

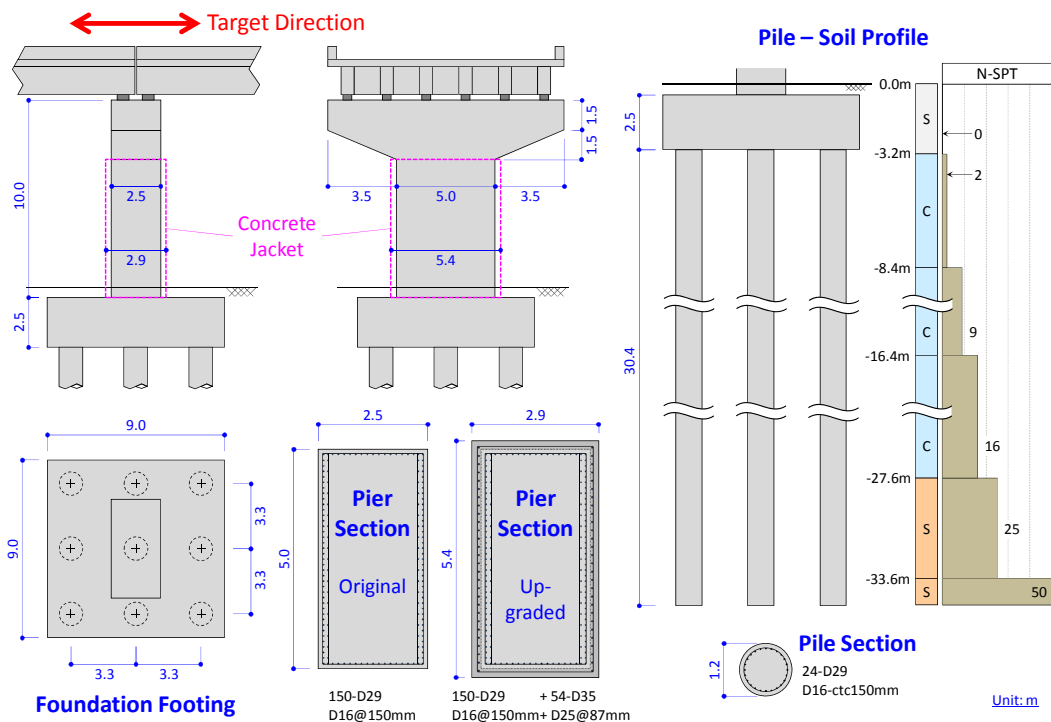


Figure 3. Target RC highway bridge pier (real-scale).

Table . Capacities of target real-scale pier before and after strengthening

<i>Real-scale pier</i>	Original pier	Strengthened pier	Upgrade ratio
Flexural capacity, MN (kips)	5.06 (1,138)	7.72 (1,736)	1.53
Shear capacity, MN (kips)	6.44 (1,448)	17.0 (3,822)	2.64
Shear-to-flexural capacity ratio	1.27	2.21	-----
Lateral capacity of foundation, MN (kips)	8.58 (1,929)	8.58 (1,929)	-----
Capacity ratio of foundation to pier	1.70	1.11	-----

S-PSD TEST WITH PIER SPECIMEN LOADING

Test cases

A S-PSD test was conducted for the 3-DOF system. Here, the restoring force in the pier spring was obtained by the pier specimen loading test, whereas forces in the foundation springs were calculated by a

simple bilinear model and Hardin-Drnevich model [8]. Test cases are summarized in Table 2. “N-S” was a combination of original pier and original foundation, and “U-S” modeled a strengthened pier with original foundation. “U-SI” simulated foundation strengthening by providing soil improvement around original foundation up to the depth of -8.4m from ground surface. Here, the standard penetration test value of the improved soil layer was assumed to be 10.

Table 2. Test cases for S-PSD test with pier specimen loading

Cases	Pier	Foundation
N-S	Original	Original
U-S	Strengthened	Original
U-SI	Strengthened	With soil improvement

Test specimens and scaling factors

Small-scale pier specimens shown in Figure 4 were used in the test. The original and strengthened scaled pier specimens were designed so that they had the same values of upgrade ratio as those of the real-scale piers shown in Table 1. The calculated design capacities are tabulated in Table 3. In order to solve an equation of motion for the real-scale pier system, pier displacement and restoring force were converted in between real-scale and small scale systems. The real-scale pier displacement obtained in the step-by-step calculation was converted to the small-scale displacement and was input to the scaled specimen. The resultant restoring force of the scaled specimen was then amplified as a real-scale restoring force. The two sets of scaling factors for both displacement and restoring force are shown in Table 4, which were given as ratios of yield displacements and yield loads.

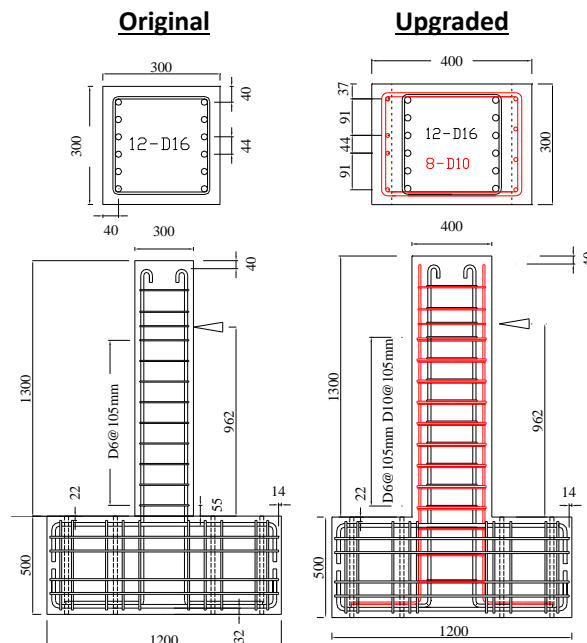


Figure 4. Scaled pier specimen details.

Table 3. Capacities of small-scaled pier specimen before and after strengthening

Small-scale pier specimen	Original pier	Strengthened pier	Upgrade ratio
Flexural capacity, kN (kips)	113 (25.4)	173 (38.9)	1.53
Shear capacity, kN (kips)	141 (31.7)	376 (84.5)	2.67
Shear-to-flexural capacity ratio	1.25	2.17	-----

Table 4. Scaling factors in terms of yield displacement and load

Scaling factors	Original pier		Strengthened pier	
	Yield disp., mm (in.)	Yield load, kN (kips)	Yield disp., mm (in.)	Yield load, kN (kips)
Real-scale pier	30.6 (1.20)	5,061 (1,138)	27.57 (1.09)	7,725 (1,737)
Scaled specimen	9.24 (0.364)	113 (25.4)	12.4 (0.488)	173 (38.9)
Scaling factor	0.3017	0.0223	0.4849	0.0229

Foundation spring parameters

Preliminary analysis of the pile foundation-soil system was conducted in order to determine the parameters of sway and rocking springs. Piles were modeled by nonlinear beam elements, and nonlinear soil reaction springs were attached to the beam elements. Sway and rocking displacements were applied to the beam-spring model and the resultant restoring forces were calculated. According to the shape of the obtained restoring force-displacement relationships, sway and rocking springs were modeled by the Hardin-Drnevich model and simple bilinear model, respectively. The determined spring parameters for the original foundation and the foundation with improved soil are tabulated in Table 5. The resultant yield load ratios of sway to pier springs were 1.69 for “N-S”, 1.11 for “U-S” and 2.06 for “U-SI”.

Table 5. Foundation spring parameters

Foundation spring parameters		Original foundation		Foundation with improved soil	
		Load, MN (kips) or Moment, MN*m (kips*ft)	Disp., cm (in.) or Rotation, rad	Load, MN (kips) or Moment, MN*m (kips*ft)	Disp., cm (in.) or Rotation, rad
Sway	Yield	8.58 (1,929)	4.6 (1.81)	15.9 (3,574)	3.1 (1.22)
	Ultimate	10.9 (2,450)	9.8 (3.86)	20.8 (4,676)	6.9 (2.72)
Rocking	Yield	264 (1.95*10 ⁵)	0.0113	281 (2.07*10 ⁵)	0.0104

Input seismic excitation

The recorded seismic acceleration wave at JMS Kobe (N-S direction) in the 1995 Kobe Earthquake, as shown in Figure 5, was selected as input seismic excitation. The peak ground acceleration (PGA) of the record was about 820 gal (323 ips²).

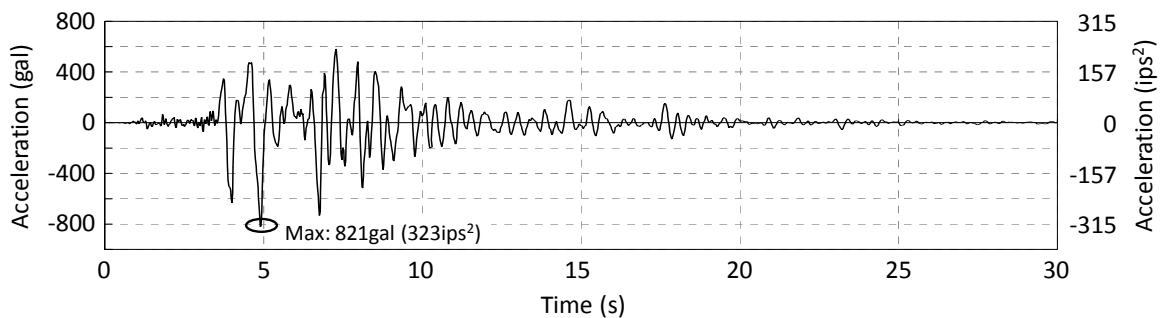


Figure 5. Input seismic excitation to 3-DOF system in the S-PSD test with pier specimen loading.

S-PSD TEST WITH FOUNDATION SPECIMEN LOADING

Test cases

An S-PSD test was also conducted for the 3-DOF system through foundation specimen loading. Here, restoring forces in the foundation springs were obtained by the foundation specimen loading test, whereas restoring force of the pier spring was calculated by a simple bilinear model. Test cases are summarized in

Table 6. “U-SN” was a combination of a strengthened pier and the original foundation, and “U-SS” simulated foundation strengthening by providing steel sheet piles and soil improvement around the original foundation.

Table 6. Test cases for S-PSD test with foundation specimen loading

<i>Cases</i>	Pier	Foundation
U-SN	Strengthened	Original
U-SS	Strengthened	Strengthened

Scaled pier-foundation system design

Compared to the pier specimen loading test cases, it was difficult to determine simple scaling factors in terms of yield load and displacement of the foundation. The precision of numerical method was needed to evaluate critical yielding load and displacement both for sway and rocking responses of the foundation. However, the applied method to evaluate them was basically for design purpose and the actual behavior of foundation was still unclear. Therefore, based on the original real-scale pier system, a small-scale system consisting of a strengthened pier and a non-strengthened foundation was designed. Because the response of the multi degree of freedom system was considered to be highly influenced by the natural periods of the system, the ratios of 2nd and 3rd natural periods to the 1st natural period were adjusted to match those of the real-scale system. The resultant configurations of the scaled system are shown in Table 7. By adjusting scaling ratios for acceleration and pier stress as 1.0 for both, those for mass, frequency, rotational inertia, pier height and pier stress became 0.01, 2.00, 0.0003, 0.09 and 0.86, respectively. The spring parameters in the 3-DOF system were determined for the designed scaled pier-foundation system.

Table 7. Configurations of real-scale and scaled 3-DOF systems for S-PSD test with foundation specimen loading

<i>Items</i>	Real-scale system	Scaled system
Top mass, kg (lb)	1,080,000 (2,380,992)	11,159 (24,601)
Footing mass, kg (lb)	486,000 (1,071,447)	5,022 (11,072)
Footing Moment of inertia, kg*m ² (lb*ft ²)	13,100,000 (310,867,721)	3,912 (92,833)
Pier cross section, m*m (in.*in.)	2.50*5.00 (8.20*16.4)	0.23*0.46 (0.755*1.51)
Pier height, m (ft.)	10.00 (32.8)	0.94 (3.08)
Natural periods, sec (Ratio to 1st period)	[1st] 0.66 (1.00) [2nd] 0.19 (0.28) [3rd] 0.08 (0.13)	[1st] 0.37 (1.00) [2nd] 0.11 (0.28) [3rd] 0.05 (0.13)

Test specimens and construction

Dimensions of the scaled foundation specimens are shown in Figure 6. Two hollow PC piles were installed into the ground by the outside-drilling method, and were connected to each other at the pile top by a concrete footing (pile cap). For the strengthened foundation specimen, soil beneath the footing was improved by cement grouting, and then steel sheet piles were penetrated into the ground around the specimen. Finally, the footing was firmly connected to the surrounding sheet piles by filling a space between them with normal concrete. The compressive strength of improved soil was 1.8MPa (261psi). The estimated capacities of the real-scale and scaled pier-foundation systems are summarized in Table 8.

The loading apparatus used in the test is shown in Figure 7. In the loading test of “U-SN”, sway and rocking displacements were simultaneously controlled through two loading jacks fixed at 0.38m (15.0in.) and 1.13m (44.5in.) high from the ground surface. In the test of “U-SS”, only one loading jack at 0.38m (15.0in.) height was used because it was considered that negligible rotation occurs during one-jack loading due to the very large rotational stiffness, as shown in Table 8.

Input seismic excitation

The recorded seismic acceleration wave shown in Figure 5 was also used; however, the wave with a duration time of 3.5sec (from 3.0sec to 6.5sec) was picked up and scaled in terms of time so that the position of the 1st natural period of the system on the response spectrum of the ground acceleration could be kept similar to that of the real-scale system. The resultant scaling ratio in the time domain was 0.50. Furthermore, the scaled acceleration wave was also amplified to a peak ground acceleration (PGA) of 1,182 gal (465 ips²) so that the input acceleration could induce a large response to the bridge.

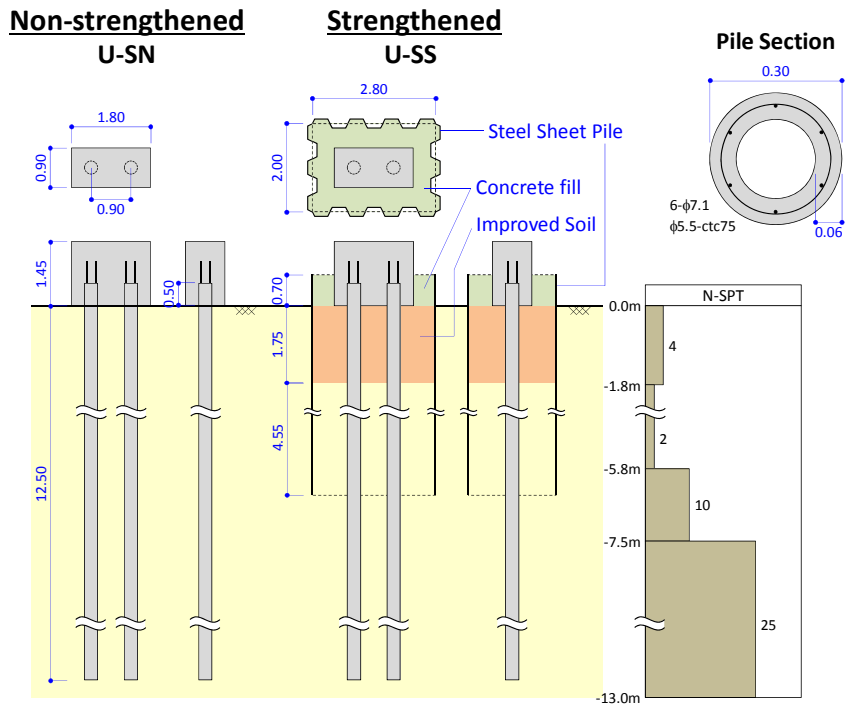


Figure 6. Configurations of foundation specimens used in the pseudo-dynamic test.

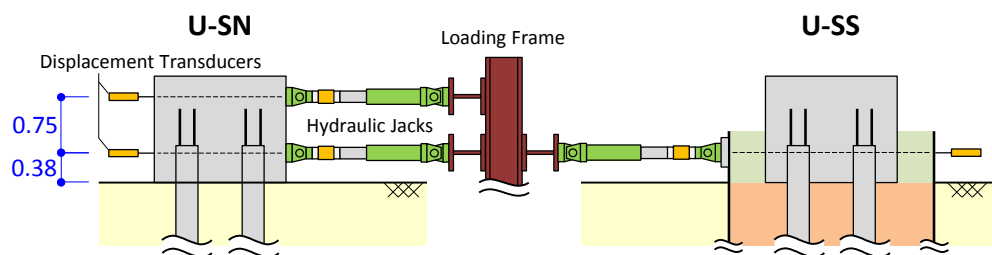


Figure 7. Arrangement of loading jacks in the pseudo-dynamic test.

TEST RESULTS AND DISCUSSION

Pier specimen loading test cases (N-S, U-S and U-SI)

Figure 8 and Figure 9 show the obtained load-displacement relationships of the pier and sway springs for the cases N-S, U-S and U-SI in the S-PSD test with pier specimen loading. Figure 10 shows the damage state of the pier specimens in the three cases at the input excitation.

Table 8. Estimated capacities of real-scale and scaled 3-DOF systems

Spring parameters		Real-scale	Scaled system	
		(non-strgt'd)	Non-strgt'd	Strengthened
Pier	Yield load, kN (kips)	5,060 (1,138)	65.7 (14.8)	131 (29.4)
	Yield disp., m (in.)	0.03 (1.18)	0.013 (0.512)	0.013 (0.512)
	Stiffness, MN/m (kips/in.)	165 (942)	4.81 (27.5)	9.61 (54.9)
Sway	Ultimate load, kN (kips)	11,220 (2,522)	126 (28.3)	838 (188)
	Ultimate disp., m (in.)	0.066 (2.60)	0.034 (1.34)	0.041 (1.61)
	Initial stiffness, MN/m (kips/in.)	415 (2,370)	13.0 (74.2)	84.3 (481)
Rocking	Ultimate moment, kN*m (kips*ft.)	172,920 (127,539)	301 (222)	938 (692)
	Ultimate rotation, rad	0.006	0.01	0.009
	Initial stiffness, MN*m/rad (kips*ft./rad)	68,591 (50,590)	64.5 (47.6)	782 (577)

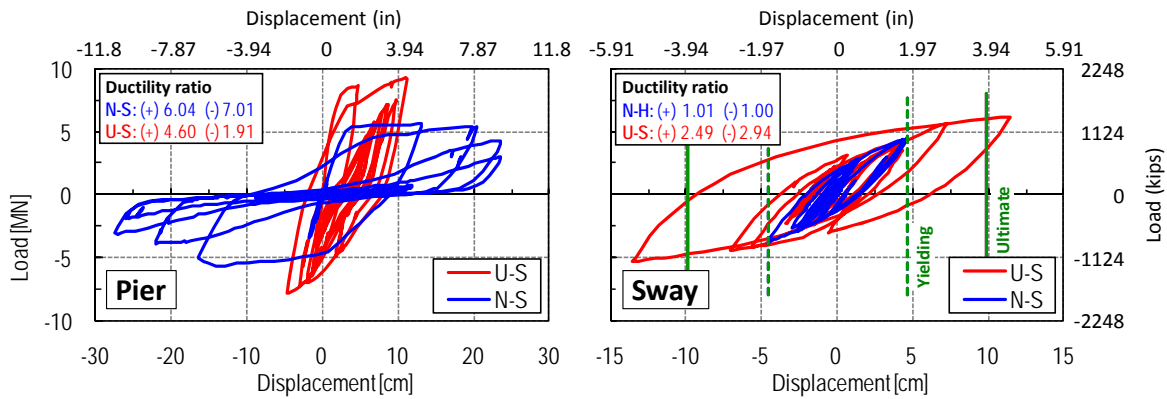


Figure 8. Load-displacement relationships of pier and sway springs (N-S vs. U-S).

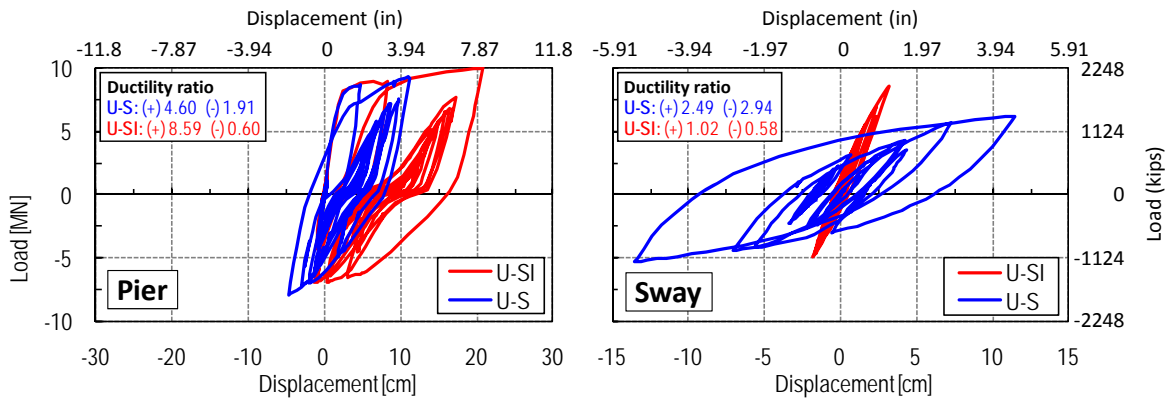


Figure 9. Load-displacement relationships of pier and sway springs (U-S vs. U-SI).

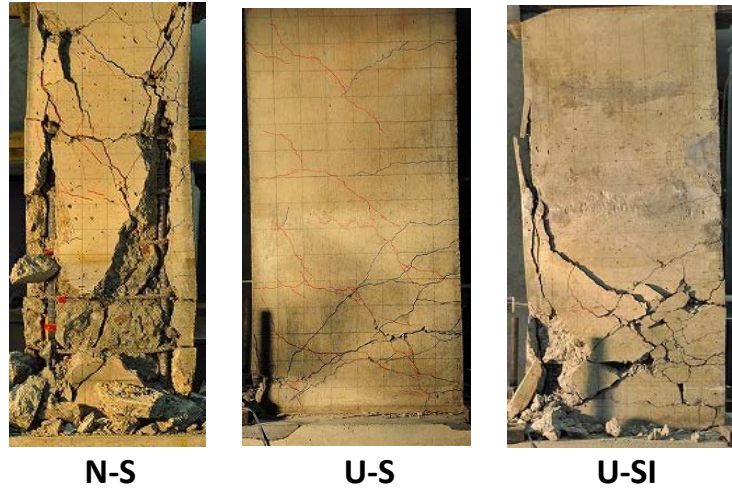


Figure 10. Damage state of the pier specimens at the end of excitation.

In N-S, very large plastic deformation and capacity degradation could be observed in the pier spring, whereas the deformation of sway spring remained less than the yield displacement. These results implied the necessity of pier strengthening.

In U-S, where the pier strengthening was provided, the pier deformation reduced within the ductility ratio of 5.0. However, the sway spring exhibited very large displacement beyond its ultimate displacement. Here, the ultimate state of pile foundation was defined as the state where sectional failure was reached in the cross sections of all piles in row perpendicular to the direction of excitation. The result showed the shift of severe damage from the pier to the foundation due to the pier strengthening.

In U-SI, where the foundation strengthening was also provided, the large plastic deformation could again be observed in the pier; however, the reduction of lateral load could not be observed because of its high capacity and ductility. According to the final state of the specimen shown in Figure 10, the damage of the pier was limited to the bottom end of the pier.

Foundation specimen loading test cases (U-SN and U-SS)

Figure 11 and Figure 12 show the obtained load-displacement relationships of the pier, sway and rocking springs in the S-PSD test with foundation specimen loading.

In U-SN (strengthened pier with original foundation), the pier response remained within its elastic range, whereas the sway response showed very large displacement. The break line in the sway diagram in Figure 11 shows the subsequent static loading test result up to the failure of the foundation specimen (pile failure) after the S-PSD test finished. The pile failure was due to breaking of internal tendons, and it was observed, by visual inspection after removal of surrounding soil, at the depth of -2.4m from ground surface. It was clarified that the maximum response displacement of the foundation specimen during the seismic excitation was very close to its ultimate displacement.

On the contrary, in U-SS (strengthened pier with strengthened foundation), the pier response was about a ductility ratio of 4.0, whereas the sway response remained in its elastic range. The subsequent static cyclic loading test result presented by the dashed line in the sway diagram in Figure 12 showed the very high capacity and ductility of the foundation specimen because of the sufficient seismic strengthening.

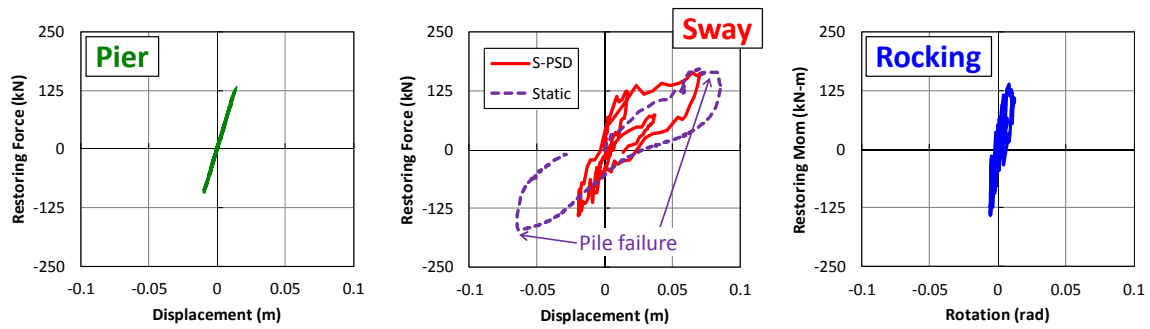


Figure 11. Load-displacement relationships of pier, sway and rocking springs (U-SN).

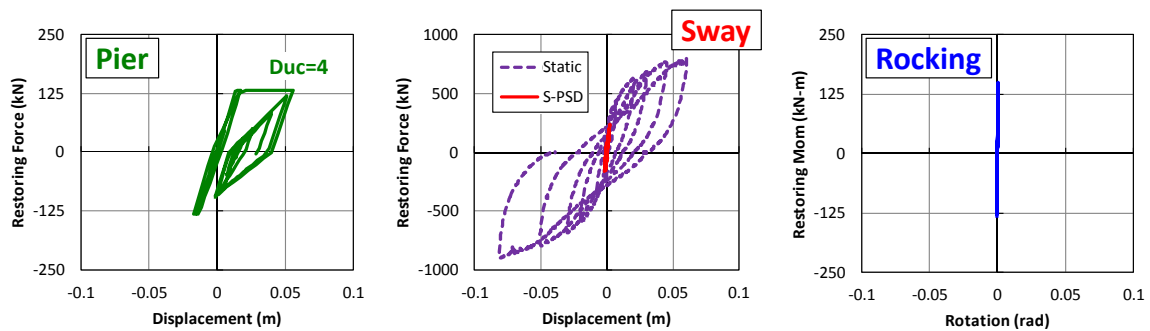


Figure 12. Load-displacement relationships of pier, sway and rocking springs (U-SS).

CONCLUSIONS

Based on the results of this experimental investigation, the following conclusions are drawn:

1. The S-PSD test with pier specimen loading showed the occurrence of severe plastic deformation of the foundation due to the enhancement in the flexural stiffness and capacity of the pier.
2. The S-PSD test with foundation specimen loading verified that foundation strengthening could efficiently prevent the seismic damage of foundation, which might occur due to pier strengthening.
3. The proposed S-PSD testing method for the superstructure-pier-foundation system could quantitatively evaluate the seismic damage in the components of the system.

ACKNOWLEDGMENTS

The authors would like to acknowledge financial support from the Grant-in-Aid for Scientific Research (B), Ministry of Education, Culture, Sports, Sciences and Technology, Japan (Representative: Hiroshi Mutsuyoshi).

REFERENCES

1. Unjoh S, Terayama T, Adachi Y, Hoshikuma J. Seismic retrofit of existing highway bridges in Japan. *Cement and Concrete Composites* 2000; 22(1):1–16.
2. Priestly NMJ, Seible F, Calvi M. *Seismic Design and Retrofit of Bridges*. Wiley: New York, 1996.
3. Mylanokis, G. and Gazetas, G., "Seismic Soil-Structure Interaction: Beneficial or Detrimental?," *J. of Earthquake Engineering*, Vol.4, No.3, 2000, pp. 277-301

4. Maki T, Maekawa K, Mutsuyoshi H. RC pile–soil interaction analysis using a 3D-finite element method with fiber theory-based beam elements. *Earthquake Engineering and Structural Dynamics* 2006; 35(13):1587–1607.
5. Chotesuwan, A., Mutsuyoshi, H. and Maki, T.: Seismic behavior of bridges with pier and foundation strengthening: PsD tests and analytical study, *Earthquake Engineering & Structural Dynamics*, Volume 41, Issue 2, pp.279-294, 2012.2
6. Nakashima, M. et al., “Integration Method Capable of Controlling Experimental Error Growth in Substructure Pseudo Dynamic Test,” *J. of Struct., Constr. Eng., AIJ*, No.454, Dec., 1993, pp. 61-71
7. Japan Road Association. *Specifications for Highway Bridges*. Japan Road Association, Japan, 1971 (in Japanese).
8. Hardin, B. O. and Drnevich, V. P., “Shear Modulus and Damping in Soils: Design Equations and Curves,” *Proc. ASCE, SM7*, 1972, pp.667-692